Developmental Biology 433 (2018) 94–107

Contents lists available at ScienceDirect

Developmental Biology

journal homepage: www.elsevier.com/locate/developmentalbiology

JNK is antagonized to ensure the correct number of interommatidial cells pattern the *Drosophila* retina

Henry L. Bushnell[a], Christina E. Feiler[a,1], Kwami F. Ketosugbo[a], Mark B. Hellerman[a], Valerie L. Nazzaro[b], Ruth I. Johnson[a,*]

[a] Biology Department, Wesleyan University, 52 Lawn Avenue, Middletown, CT, USA
[b] Quantitative Analysis Center, Wesleyan University, 222 Church Street, Middletown, CT, USA

ARTICLE INFO

Keywords:
Drosophila eye
JNK signaling
Apoptosis
Epithelial morphogenesis
Cindr
CD2AP
CIN85

ABSTRACT

Apoptosis is crucial during the morphogenesis of most organs and tissues, and is utilized for tissues to achieve their proper size, shape and patterning. Many signaling pathways contribute to the precise regulation of apoptosis. Here we show that Jun N-terminal Kinase (JNK) activity contributes to the coordinated removal of interommatidial cells via apoptosis in the *Drosophila* pupal retina. This is consistent with previous findings that JNK activity promotes apoptosis in other epithelia. However, we found that JNK activity is repressed by Cindr (the CIN85 and CD2AP ortholog) in order to promote cell survival. Reducing the amount of Cindr resulted in ectopic cell death. Increased expression of the *Drosophila* JNK *basket* in the setting of reduced *cindr* expression was found to result in even more severe apoptosis, whilst ectopic death was found to be reduced if retinas were heterozygous for *basket*. Hence Cindr is required to properly restrict JNK-mediated apoptosis in the pupal eye, resulting in the correct number of interommatidial cells. A lack of precise control over developmental apoptosis can lead to improper tissue morphogenesis.

1. Introduction

The removal of cells by apoptosis is a fundamental feature of tissue and organ morphogenesis, homeostasis and pathogenesis (Fuchs and Steller, 2011). During development, apoptosis is utilized for the strategic removal of cells to sculpt organs and tissues. Further, the shrinking of apoptotic cells can exert pulling forces on their neighbors and contribute to overall tissue shape (Teng and Toyama, 2011). In addition, apoptosis removes normal cells that have been generated in excess and abnormal cells before these can compromise a tissue.

Multiple mechanisms have evolved to keep apoptosis in check. First, activation of the caspases – conserved cysteine proteases that execute apoptosis – is a multistep process. In *Drosophila melanogaster*, these caspases include the initiator caspases Death-related ced-3/Nedd2-like caspase (Dredd) (Chen et al., 1998) and Death regulator Nedd2-like caspase (Dronc) (Dorstyn et al., 1999) that activate the executioner caspases Death related ICE-like caspase (Drice) (Fraser and Evan, 1997; Fraser et al., 1997) and Death caspase 1 (Dcp-1) (Song et al., 1997). Death-associated inhibitor of apoptosis 1 (Diap1) is widely expressed in *Drosophila* tissues and binds directly to apoptotic caspases to inhibit their activity (Hawkins et al., 1999; Hay et al., 1995; Vucic et al., 1997, 1998). Diap1 also contains E3 ligase activity that directs ubiquitination of Dronc, leading to its degradation (Wilson et al., 2002). In response to apoptotic stimuli that include developmental and stress signals, the RHG proteins, Reaper (Rpr), Head involution defective (Hid) and Grim bind Diap1, promoting its degradation (Bergmann et al., 1998; Chen et al., 1996; Goyal et al., 2000; Grether et al., 1995; Lisi et al., 2000; Ryoo et al., 2002; Wang et al., 1999; White et al., 1994; Wilson et al., 2002). In addition, stress and developmental signals modify expression of *Diap1*, the RGH loci and *Dronc*. For instance, expression of RGH loci is stimulated by *Drosophila melanogaster* p53 (Dmp53P) following DNA damage (Brodsky et al., 2000) and by ecdysone signaling during pupal metamorphosis (Jiang et al., 2000; Robinow et al., 1997). Conversely, *hid* expression is repressed downstream of Epidermal growth factor receptor (EGFR) activity (Kurada and White, 1998) whilst *Diap1* expression is promoted by the pro-survival transcriptional activator Yorkie (Huang et al., 2005) and STAT92E, a stress-activated transcription factor of the Jak-STAT pathway (Betz et al., 2008). In addition, direct phosphorylation of Hid by the mitogen-activated protein kinase (MAPK) Rolled that is activated downstream of the EGFR inhibits Hid activity to promote cell survival (Bergmann et al., 1998, 2002).

The *Drosophila* eye has been an indispensable tool for analyses of the

* Corresponding author.
E-mail address: rijohnson@wesleyan.edu (R.I. Johnson).
[1] Present address: Technische Universitaet Muenchen, WZW, Emil-Ramann-Strasse 2, 85354 Freising-Weihenstephan, Germany.

https://doi.org/10.1016/j.ydbio.2017.11.002
Received 27 June 2017; Received in revised form 29 October 2017; Accepted 4 November 2017
Available online 11 November 2017

apoptotic caspases and their regulators. It is an excellent model in which to examine the developmental signals that regulate apoptosis because death of surplus interommatidial cells (ICs) - epithelial cells that separate ommatidia - occurs within an 18-h period of mid-pupal development that is accessible to genetic manipulation and imaging (Cagan and Ready, 1989b). Additionally, the pupal retina is post-mitotic and even experimental manipulations that significantly increase apoptosis do not trigger apoptosis-induced compensatory proliferation (reviewed by Fuchs and Steller (2015)). Hence the consequences of experimental manipulations of apoptosis can be accurately quantified.

After apoptosis has ceased in the retina, a precise number of ICs surround each ommatidium, indicating the presence of mechanisms that ensure neither too many nor too few ICs are removed. The precise nature of this mechanism remains elusive, but it likely relies on a surge of 20-hydroxyecdysone that roughly coincides with the death of most ICs (Riddiford, 1993; Yin and Thummel, 2005) and the integration of developmental signals that promote or repress IC apoptosis. These signals include EGFR activity, which confers IC survival, and Notch and Wingless (Wg) which are required for IC death (Baker and Yu, 2001; Cagan and Ready, 1989b; Cordero et al., 2004; Miller and Cagan, 1998; Parks et al., 1995). Intriguingly, the position of an IC can determine whether it survives or not. ICs close to differentiating bristle groups are most likely to die, whilst ICs in contact with more than two primary pigment cells (1°s) are most likely to survive (Monserrate and Brachmann, 2007; Wolff and Ready, 1993). Hence positional information across the retina determines cell death/survival decisions, but how this information is encoded has not been clearly resolved. Differences in Notch or EGFR activities do not appear to correlate with cell death or survival (Monserrate and Brachmann, 2007), suggesting the integration of additional molecular mechanisms that confer susceptibility or resilience to apoptosis.

Here, we explore whether activity of the Jun-N-terminal Kinase pathway (JNK) is regulated to ensure correct elimination of ICs from the *Drosophila* pupal eye. JNK activity can promote apoptosis, although this context-dependent output has been mainly associated with a stress response (Craige et al., 2016; Hotamisligil and Davis, 2016). For instance, JNK is activated in response to DNA damage, leading to elevated expression of *hid* via JNK-mediated activation of the AP-1 transcription factors (Luo et al., 2007). JNK is also activated in response to disruption of the Cdc42-Par6-atypical protein kinase C complex, which is essential for epithelial cell polarity, leading to epithelial cell death (Warner et al., 2010). Activation of JNK in dying epithelial cells can lead to morphogen expression that induces proliferation of other cells to maintain tissue size, or secretion of Eiger, the ligand of the *Drosophila* tumor necrosis factor receptor (TNFR) that triggers JNK signaling leading to additional cell death (Fuchs and Steller, 2015). In addition, JNK signaling can be activated downstream of Dronc, resulting in a positive feedback loop that amplifies the robustness of apoptosis (Shlevkov and Morata, 2012).

In *Drosophila*, JNK signaling is characterized by the sequential phosphorylation of a cascade of conserved kinases. These include the JNK Basket (Bsk) (Riesgo-Escovar et al., 1996; Sluss et al., 1996) that is activated by the JNKK Hemipterous (Hep) (Glise et al., 1995), which is in turn activated by the JNKKKs Slipper (Slpr) (Sathyanarayana et al., 2003; Stronach and Perrimon, 2002), Mekk1 (Chen et al., 2002; Inoue et al., 2001), TAK1 (Silverman et al., 2003; Takatsu et al., 2000) or ASK1 (Chen et al., 2002; Kuranaga et al., 2002). The JNKKKs are activated by the Ste20-related kinase Misshapen (Msn) (Su et al., 1998), the TNFR-associated factors TRAF1 and TRAF2 (Cha et al., 2003; Kuranaga et al., 2002; Liu et al., 1999) or small GTPases (Chen et al., 2002; Teramoto et al., 1996). Phosphorylated Bsk activates the transcription factors Jra (Riesgo-Escovar et al., 1996; Sluss et al., 1996) and Kay (Zeitlinger et al., 1997), the *Drosophila* orthologs of Jun and Fos, respectively. Activity of these AP-1 transcription factors can result in apoptosis or changes in cell shape and motility that are especially important for morphogenesis (Rios-Barrera and Riesgo-Escovar, 2013). The phosphatase Puckered (Puc), which is a transcriptional target of Jun/Fos, regulates JNK signaling by inactivating Bsk (Martin-Blanco et al., 1998).

We recently described that the conserved adaptor protein Cindr complexes with Bsk to limit JNK signaling in wing epithelia (Yasin et al., 2016). Cindr is also essential for patterning of the pupal eye, where it regulates the localization of adhesion receptors and the actin cytoskeleton, structures that must be appropriately remodeled for ICs to acquire appropriate positions and shapes (Johnson et al., 2012, 2011, 2008). There are two vertebrate orthologs of Cindr: CD2-associated protein (CD2AP) and Cbl-interacting protein of 85 kDa (Cin85) (Bogler et al., 2000; Dustin et al., 1998; Gout et al., 2000; Kirsch et al., 1999; Lehtonen et al., 2000; Take et al., 2000). CIN85 has mainly been associated with clathrin-mediated endocytosis of receptor tyrosine kinases (RTKs) and transmembrane receptors (Kowanetz et al., 2004; Szymkiewicz et al., 2002; Tossidou et al., 2010). CD2AP plays an especially important role in maintaining the slit diaphragm, a specialized junction that links podocyte foot processes in kidney glomeruli (Faul et al., 2007; Kawachi et al., 2006). CD2AP is also important for podocyte survival and this has been ascribed to interactions between CD2AP and phosphoinositide-3-kinase (PI3-K)/Akt signaling as well transforming growth factor-β (TGF-β) activity (Asanuma et al., 2007; Huber et al., 2003; Schiffer et al., 2004).

Here, we describe that Cindr, in addition to its other roles in the developing pupal eye epithelium, regulates the survival of epithelial cells in the *Drosophila* pupal retina by limiting JNK activity. When we reduced expression of Cindr, JNK activity was enhanced and triggered the removal of a large number of ICs, an effect that was reversed when JNK signaling was compromised. Cindr is richly expressed in the eye retina, which we hypothesize provides a mechanism for widespread JNK repression. However, Cindr neither limits Bsk concentrations nor its phosphorylation. In addition, our genetic data suggest that at least some JNK signaling is still activated during IC death, despite the presence of Cindr. Finally, modifying Cindr and JNK signaling potential introduced defects in the positioning of ICs, indicating that a low level of JNK activity in the retina contributes to IC patterning.

2. Materials and methods

2.1. Drosophila genetics

The progeny of all crosses were cultured at 25 °C until dissection or processing. We used *GMR-GAL4* (Bloomington stock center, BL-1104), *da-GAL4* (BL-5460), *c765-GAL4* (BL-36523) and *pnr-GAL4* (BL-3039) to drive transgene expression in the developing larval and pupal eye, embryo, larval wing, and pupal thorax respectively. UAS transgenes were *UAS-bsk* (BL-9310), *UAS-bsk^{DN}* (BL-6409), *UAS-bsk^{RNAiGL00431}* (BL-35594), *UAS-bsk^{RNAiJF01275}* (BL-31323), *UAS-hep^{RNAiGL00089}* (BL-28710), *UAS-jun^{RNAiJF01184}* (BL-31595). *UAS-msn^{RNAiJF03219}* (BL-28791), *UAS-puc* (gift from R.L. Cagan), *UAS-slpr$^{KD9+DK13}$* (BL-58799), *UAS-cindr$^{RNAi2.21+23}$* which we abbreviate to *UAS-cindr^{RNAi-2}* (described in Johnson et al. (2008)), *UAS-cindr^{GFP}* (described in Johnson et al. (2008)), *UAS-GFP* (BL-6874) and *UAS-lacZ*. JNK activity was assayed via expression of the *puc^{E69}* enhancer trap (gift from R.L. Cagan). Alleles used were *bsk^{1}* (BL-3088), *bsk^{2}* (BL-108149), *fos^{1}* (*kay^{1}*) and *fos^{2}* (*kay^{2}*, gifts from U. Weber), *hep^{r75}* (BL-6761), *jun$^{76\text{-}19}$* (*jra$^{76\text{-}19}$*) and *jun^{A109}* (*jra^{A109}*, gifts from U. Weber).

2.2. Dissection, immunofluorescence and microscopy

Retina were dissected from pupae collected at 0 h APF and maintained at 25 °C until dissection, or wandering third instar larvae, in ice-cold PBS and fixed in 4% formaldehyde. Primary antibodies were rat anti-DE-Cad2 (1:20, DSHB), rat anti-Elav (1:20, DSHB), mouse anti-β-Galactosidase (1:20, DSHB), rabbit anti-cleaved Dcp-1 (1:100, Cell Signaling) and rabbit anti-phospho Histone3 (1:200, Upstate

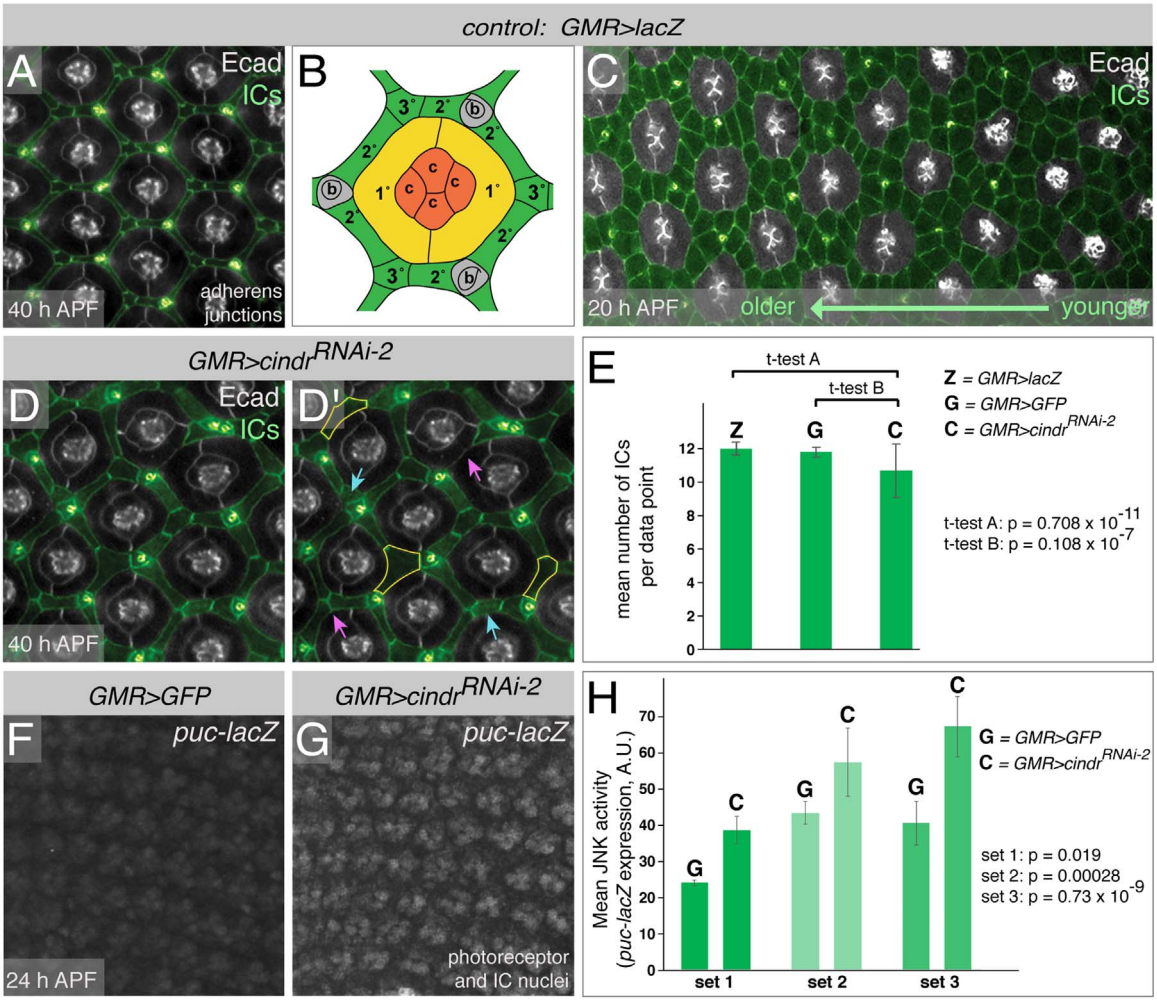

Fig. 1. Eye patterning requires Cindr, which represses JNK signaling activity. (A) Small region of the *Drosophila* eye at 40 h APF. ICs are pseudo-colored green in this and all other images. (B) Cartoon of an individual ommatidium with cone cells (c) in orange, 1° cells in yellow, 2° and 3° IC cells in green and bristle groups (b) in grey. (C) At 20 h APF a marked gradient of development characterizes the eye; ICs are more disorganized in younger tissue (to the right). (D) Expression of *UAS-cindr*$^{RNAi-2}$ disrupts the ordered pattern of the retina and reduces the number of ICs. (D') Examples of cells that expand to occupy multiple niches are outlined in yellow, pink arrows indicate positions of missing cells, blue arrows indicate cells that are incorrectly positioned. (E) IC number in control retinas expressing *lacZ* and *GFP*, and retinas expressing *cindr*$^{RNAi-2}$. Error bars indicate standard deviation. Two-sample t-tests compared IC numbers in *GMR > cindr*$^{RNAi-2}$ and control retinas as indicated. (F) *puc-lacZ* expression in control retinas and (G) in response to *UAS-cindr*$^{RNAi-2}$ expression. See Fig. S2 for additional examples of *puc-lacZ* expression in retinas. (H) Mean *puc-lacZ* expression, measured as β-galactosidase fluorescence intensity, in three independent sets of retinas with ectopic *GFP* or *cindr*$^{RNAi-2}$ expression. Two-sample t-test p-values that compared β-galactosidase fluorescence in each set of control and experimental retinas are indicated. Error bars plot standard deviation.

Biotechnology). Secondary antibodies were conjugated Alexafluor 488 or Cy3 (Jackson ImmunoResearch). Retinas were imaged with a Zeiss LSM 501 confocal and associated Zen software or Leica TCS SP5 DM fluorescence microscope and associated LAS AF software. Adult thoraces were imaged with a Leica M125 stereo-dissecting microscope, Leica IC80HD camera and Leica Acquire software. All images were prepared for publication using Adobe Photoshop: images were aligned and cropped; minimal and equal adjustments were applied to images of control and experimental retinas; pseudo-color was introduced to highlight all ICs.

2.3. Image analysis

To quantify the number of ICs, hexagonal data-points were drawn by joining six ommatidia surrounding a single ommatidium, as illustrated in Fig. S1 and all ICs enclosed within these data-points were counted. Since 1° cells and bristle groups are recruited from the pool of ICs between ~17 to 22 h APF, these were included in cell counts of 18, 21, 24 and 27 h APF retinas. Between 6 and 8 retinas were assessed for each genotype per age APF and the cells counted in 7 to 15 data points per eye. Only the central third of each retina was analyzed as the retina is characterized by a developmental gradient.

The severity of cell death was scored by assessing the amount of cleaved Dcp-1 observed in whole retinas dissected at 18, 21, 24 and 27 h APF. Each retina was scored to be exhibiting mild cell death (retinas with a low number of Dcp-1 positive cells, eg. Fig. 2B), moderate death (retina characterized by moderate Dcp-1 activity across the eye field, eg. Fig. 2E), severe death (a large number of cells that were Dcp-1 positive, eg. Fig. S4D). Damaged regions of retinas were excluded from analyses. Between 13 and 39 retinas were assessed for each genotype per age APF.

Expression of the *puc*^{E69} enhancer trap, a proxy for JNK signaling activity, was assessed by detecting β-Galactosidase in *GMR > GFP* and *GMR > cindr*$^{RNAi2.21+23}$ retinas dissected at 24 h APF. Retinas of both genotypes were dissected consecutively and processed using common solutions. Confocal imaging and analyses utilized identical parameters. To analyze fluorescence intensity of *β-galactosidase* expression, ImageJ 1.50i was used to measure the mean grey value of grayscale maximal projection images generated from the same number of serial confocal sections. Three or four retinas of each genotype were analyzed for each of the three independent data sets (analyses are presented in Fig. 1H which plots mean fluorescence intensities). Regions of retinas that had been damaged during dissection and regions of *GMR > cindr*$^{RNAi2.21+23}$ retinas

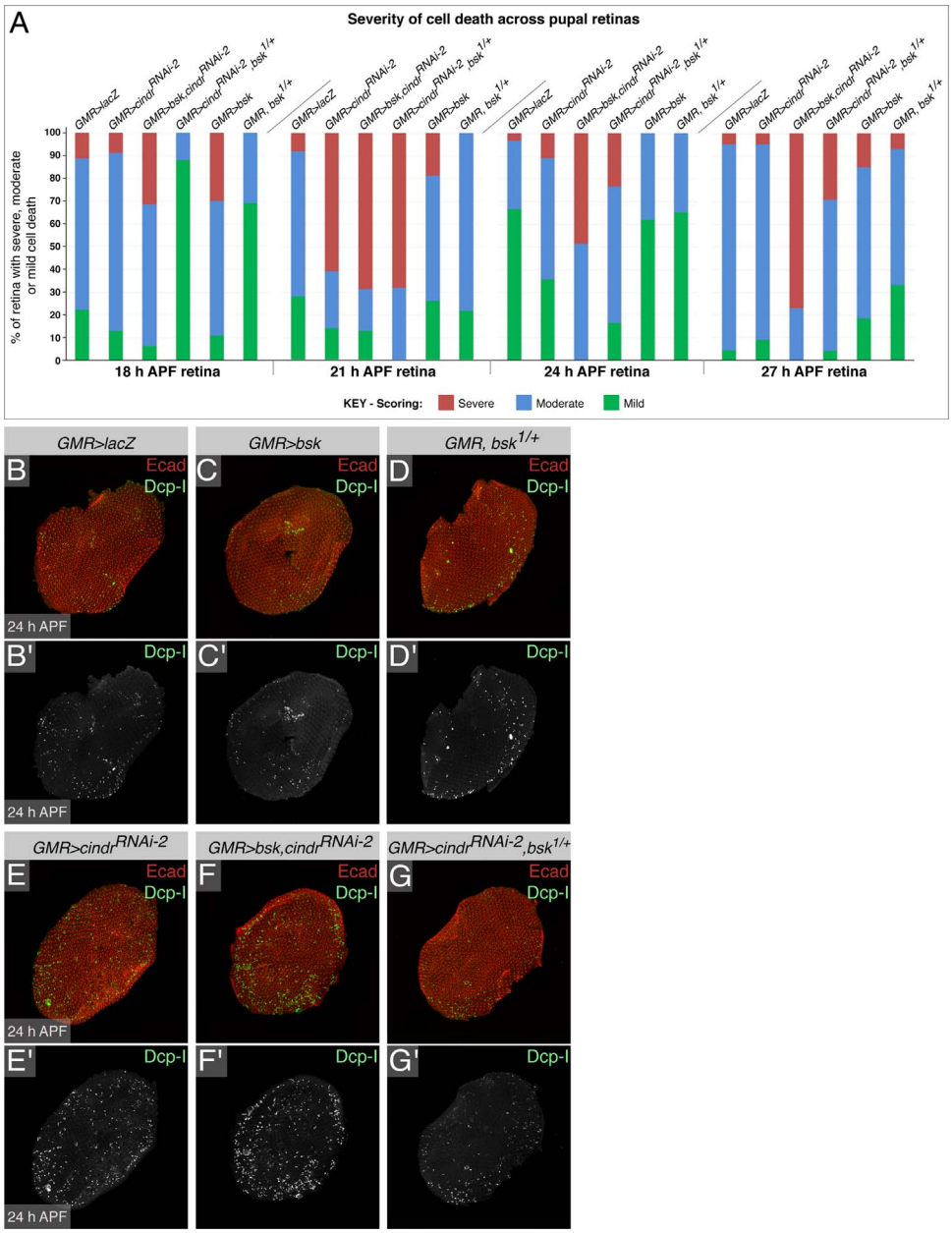

Fig. 2. Apoptosis in the retina is modified by Cindr and JNK. (A) Proportion of retinas characterized by severe, moderate or mild amounts of cell death (assessed via Dcp-1 activation, see Section 2) at 18 h, 21 h, 24 h and 27 h APF. (B-G) Examples of retinas characteristic of each genotype at 24 h APF. Retinas of other ages are presented in Figs. S3, S4 and S5. Dying cells were detected with an antibody to activated Dcp-1. Dcp-1 and ECad are shown in panels B-G and Dcp-1 only in B'-G'.

that were marked by small 'holes' (probably due to severe apoptosis) were excluded from analyses as such damage could trigger stress- or repair-induced JNK activity. Examples of images analyzed are presented in Fig. S2, with regions analyzed marked.

Patterning errors were assessed and quantified as previously described (Johnson and Cagan, 2009). Briefly, all patterning errors observed within hexagonal data points were counted and the mean ommatidial mis-patterning scores calculated from 75 data points per genotype.

2.4. Western blotting and analysis

Embryo lysates were prepared from embryos of genotypes *da > GFP*, *da > cindr^{GFP}* and *da > cindr^{RNAi2}*. 100 µL of embryos of each genotype were aged between 5 and 10 h after egg laying, dechorionated and crushed in lysis buffer: 20 mM HEPES at pH 7.5 with 125 mM NaCl, 1.5 mM $MgCl_2$, 1 mM EDTA, 1 mM DTT, 1 mM Na_3VO_4, 1 mM β-glycerolphosphate, 25 mM NaF, cOmplete™ protease inhibitor cocktail (Roche) and 20% glycerol. The lysate was cleared with centrifugation for 1 min at 5500 rpm and frozen. Three independent samples of embryo lysate were prepared for each of the three genotypes. Each lysate sample was analyzed via SDS-PAGE and Western Blotting at least three times. Wing discs from 24 wandering third larval instar larvae of genotypes *c765 > GFP*, *c765 > cindr^{GFP}* and *c765 > cindr^{RNAi2}* were dissected in ice-cold PBS supplemented with 1 mM DTT, 1 mM Na_3VO_4, 1 mM β-glycerolphosphate, and cOmplete protease inhibitor cocktail (Roche). The wing discs were transferred to 25uL lysis buffer (as before). Each sample was analyzed by SDS-PAGE and Western Blotting three times.

Western Blots were probed with rabbit anti-Cindr (1:500, Johnson et al., 2008), Rabbit anti-JNK (1:500, Santa Cruz Biotechnology), Rabbit anti-phospho-JNK (1:700, Cell Signaling Technology) and goat anti-GAPDH (1:3000, Imgenex) as a loading control. LICOR Image Studio Software was utilized for densitrometry analyses to quantify

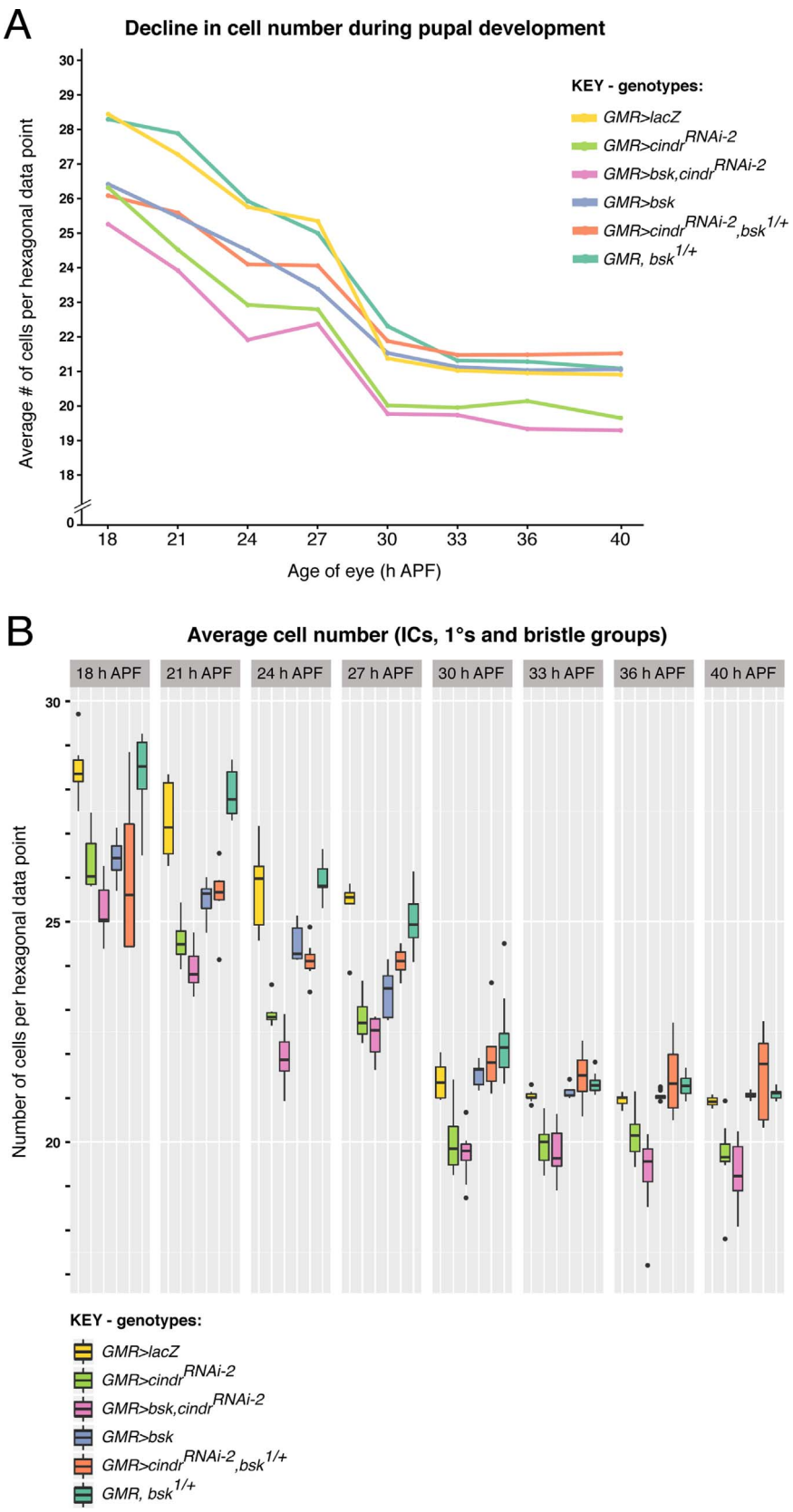

Fig. 3. Modifying *cindr* expression and JNK activity modifies the removal of cells from pupal retinas. (A) Graph depicting mean number of cells (plotted as a line) in retinas analyzed between 18 and 40 h APF (see Section 2). (B) Box and whisker plots of number of cells in retinas for each genotype at all seven ages APF. Points represent outliers within each genotype. See Fig. S7 for further statistical analyses determining differences between each genotype at each age.

relative quantities of JNK (Fig. 6B and D), pJNK (Fig. 6D) and Cindr (not shown).

2.5. Statistical analyses

Two-sample *t*-tests were used to assess differences between JNK activity (*puc-lacZ* expression, Fig. 1E), cell number (Fig. 1H, Table 2, Table 3), ommatidial mis-patterning scores (Table 4), total JNK and pJNK (Fig. 6B and D). One-way ANOVA tests were used to compare genotype on the number of cell counts at 18, 21, 24, 27, 30,33, 36 and 40 h APF (ages were considered separately), each at significance level 0.05 (Fig. S7A). Post-hoc analyses using the Tukey procedure revealed which genotypes varied significantly (Fig. S7B).

3. Results

3.1. Cindr is required for the proper survival of ICs in the Drosophila pupal eye

The *Drosophila* eye is striking in its order. Each ommatidium, with its core of eight photoreceptor neurons encapsulated by four cone cells and a pair of primary pigment cells (1°s), is separated by pigment-producing interommatidial cells (ICs) arranged in a precise honeycomb lattice that spans the eye field (Fig. 1A and B) (Cagan, 1993; Cagan and Ready, 1989a; Wolff and Ready, 1993). Six secondary pigment cells (2°s) form the sides of each hexagonal unit. Bristle groups and tertiary pigment cells (3°s) occupy alternate corners of the hexagon (Fig. 1A and B). This distinctive cellular arrangement arises when the organism is a pupa and requires the integration of a variety of signals and cell behaviors.

The early pupal retina is characterized by a developmental gradient. At 20 h after puparium formation (APF), ICs are untidily arranged between ommatidia in the younger, anterior part of the eye, but rearrange into single file and progressively adopt smaller, more ordered shapes (Fig. 1C). The early pupal retina is characterized by a large number of superfluous ICs. These are removed by apoptosis, leaving the precise number of cells that adopt characteristic 2° and 3° cell shapes by 40 h APF (Fig. 1A) (Cagan and Ready, 1989b).

Reducing *cindr* expression during pupal eye patterning compromised the arrangement and shape of many ICs, largely due to disruptions to adhesive junctions and the cytoskeleton during patterning (Johnson et al., 2012, 2011, 2008). These disruptions lead to classic rough-eye phenotypes in *GMR > cindr^{RNAi}* adults (not shown, (Johnson et al., 2008)). In addition, expression of *UAS-cindr$^{RNAi\text{-}2}$* transgenes that reduce expression of Cindr isoforms that contain SH3 domains (Johnson et al., 2008), also decreased the number of ICs within the eye field (Fig. 1D). To quantify this defect in IC survival, we compared the number of ICs within hexagonal 'data points' delineated by connecting the centers of six ommatidia (illustrated in Fig. S1A and B). In control retinas expressing *green fluorescent protein* (*GFP*) or *β-Galactosidase* (encoded by *lacZ*), an average of 12.1 and 11.9 cells lay within each data point, respectively (Fig. 1E). Wild type *Canton S* retinas are similarly characterized by ~12 ICs per data point (not shown). However, reducing *cindr* decreased this number to 10.8 cells (Fig. 1E) reflecting a significant change in the regulated removal of ICs. These data suggest that Cindr counteracts cell death to ensure a suitable number of ICs remain within the IC lattice.

3.2. JNK activity is repressed by Cindr in pupal retinas

Recently, we reported that Cindr interacted with the *Drosophila* JNK Basket (Bsk) in the wing epithelium (Yasin et al., 2016). This interaction was crucial to preserve epithelial integrity: loss of *cindr* increased JNK signaling that triggered extensive cell delamination and apoptosis (Yasin et al., 2016). Since Cindr is richly expressed in the pupal retina (Johnson et al., 2008), we posited that one role for Cindr would be to similarly oppose JNK signaling during eye patterning. Supporting this hypothesis, expression of *puc-lacZ* (*puc^{E69}*), a read-out of JNK signaling activity (Ring and Martinez Arias, 1993), was increased in the retina when *cindr* was reduced (Fig. 1F-H, Fig. S2).

3.3. Cindr inhibits JNK activity to promote survival of ICs

Apoptosis removes surplus ICs from the pupal retina as the lattice is patterned (Cagan and Ready, 1989b; Wolff and Ready, 1993). To directly assay the contributions of Cindr and JNK to cell death, we examined the activation of Death caspase-1 (Dcp-1) when Cindr and JNK activity were modified (Fig. 2). As a second measure, we counted the cells that lay within hexagonal data points (Fig. 3). Since 1° cells are recruited from the pool of interommatidial cells from ~18 through ~23 h APF we included these in our cell counts (although their numbers did not vary significantly between the genotypes we examined at any time point, data not shown). Bristle groups were also included, as these originate from cells selected from the IC pool from ~ 16 h APF. Our strategy for counting cells in these young retinas is illustrated in Fig. S1C and D.

In control retinas expressing *lacZ*, we observed a mean decline of 7.36 cells, per data point, from 18 h APF to 40 h APF (Table 1, Fig. 3A). Cell counts confirmed that this decline is not steady, but characterized by two periods of enhanced apoptosis: from 21 to 24 h APF and from 27 to 30 h APF (Table 1). Few cells were removed after 30 h APF. These data were similar to previous characterizations of the loss of ICs from pupal retinas (Cagan and Ready, 1989b; Monserrate and Brachmann, 2007), although note that the retinas analyzed by Cagan and Ready were raised at 20 °C rather than 25 °C in this study and hence developed at a slower pace. Dcp-1 activity was enhanced at the anterior periphery of the eye field at 18 h APF, as previously observed (Wolff and Ready, 1993), and apoptotic cells were also dispersed through the entire retina (Fig. S3A). Ranking Dcp-1 activity into one of three categories (mild, moderate or severe, reflecting the amount of Dcp-1

Table 1
Loss of cells from retinas during pupal development.[a]

Genotype	Mean change in cell number[b]							Total cells lost from 18 to 40 h APF
	18 to 21 h APF	21 to 24 h APF	24 to 27 h APF	27 to 30 h APF	30 to 33 h APF	33 to 36 h APF	36 to 40 h APF	
GMR > lacZ	−0.97	−1.54	−0.42	−3.90	−0.41	−0.08	−0.04	**7.36**
GMR > cindr^{RNAi}	−1.80	−1.58	−0.15	−2.77	−0.09	0.17	−0.49	**6.71**
GMR > cindr^{RNAi}, bsk (overexpression)	−1.24	−1.99	0.26	−2.41	−0.04	−0.36	−0.09	**5.87**
GMR > cindr^{RNAi}, bsk$^{1/+}$	−0.72	−1.43	−0.13	−2.19	−0.27	−0.07	0.05	**4.76**
GMR > bsk (overexpression)	−0.82	−1.07	−1.09	−1.90	−0.41	−0.07	0.01	**5.35**
GMR, bsk$^{1/+}$	−0.38	−1.96	−0.89	−2.90	−0.82	−0.04	−0.19	**7.18**

[a] Interommatidial cells, 1° cells, and bristle groups were included in cell-counts (see Fig. S1C).
[b] For each genotype, mean values were calculated from analyses of 67 to 160 data points distributed across 10 to 16 independent retinas.

Table 2
Quantification of the number of ICs in retinas at 40 h APF (N=75).

GENOTYPE	nature of transgene/allele (if known)	IC number per data point Mean [1.]	SD	p-value [2.]
GMR>lacZ	overexpression	12.1	0.4	
GMR>GFP	overexpression	11.9	0.3	
GMR>cindr^{RNAi}	RNAi	**11.0**	1.2	1.81 x 10^{-4}
GMR>cindr^{RNAi}, bsk		**9.7**	1.1	
GMR>bsk	overexpression	12.0	0.5	
GMR>cindr^{RNAi}		**11.2**	1.6	4.77 x 10^{-4}
GMR>cindr^{RNAi}, msn$^{102/+}$		**12.2**	1.8	
GMR, msn$^{102/+}$	loss of function	12.0	0.3	
GMR>cindr^{RNAi}		**10.7**	1.3	6.68 x 10^{-18}
GMR>cindr^{RNAi}, slpr$^{BS06/+}$		**13.6**	2.2	
GMR, slpr$^{BS06/+}$	loss of function	12.2	0.4	
GMR>cindr^{RNAi}		**10.0**	2.0	5.86 x 10^{-7}
GMR>cindr^{RNAi}, hep$^{r75/+}$		**11.0**	1.2	
GMR, hep$^{r75/+}$	amorphic	12.0	0.3	
GMR>cindr^{RNAi}		**10.6**	1.5	6.19 x 10^{-7}
GMR>cindr^{RNAi}, bsk$^{1/+}$		**12.5**	2.7	
GMR, bsk$^{1/+}$	mutation in substrate recognition region, loss of function	**12.0**	0.0	
GMR>cindr^{RNAi}		**10.5**	1.4	1.32 x 10^{-18}
GMR>cindr^{RNAi}, bsk$^{2/+}$		**14.6**	3.0	
GMR, bsk$^{2/+}$	mutation in kinase domain, loss of function	12.0	0.1	
GMR>cindr^{RNAi}		**10.2**	1.1	1.38 x 10^{-2}
GMR>cindr^{RNAi}, jun$^{76-19/+}$		**10.8**	1.6	
GMR, jun$^{76-19/+}$	amorphic	11.9	0.3	
GMR>cindr^{RNAi}		**11.0**	1.6	2.90 x 10^{-7}
GMR>cindr^{RNAi}, jun$^{A109/+}$		**11.9**	2.1	
GMR, jun$^{A109/+}$	amorphic	12.0	0.4	
GMR>cindr^{RNAi}		**10.1**	1.0	9.19 x 10^{-7}
GMR>cindr^{RNAi}, fos$^{1/+}$		**11.1**	1.5	
GMR, fos$^{1/+}$	amorphic	**12.0**	0.4	
GMR>cindr^{RNAi}		**10.4**	1.2	1.39 x 10^{-5}
GMR>cindr^{RNAi}, fos$^{2/+}$		**11.5**	1.7	
GMR, fos$^{2/+}$	hypomorphic	12.0	0.3	
GMR>cindr^{RNAi}		**10.4**	1.3	1.9 x 10^{-2}
GMR>cindr^{RNAi}, jun$^{76-19/+}$, fos$^{1/+}$		**11.2**	1.8	
GMR, jun$^{76-19/+}$, fos$^{1/+}$	amorphic, amorphic	12.2	0.5	

1. Mean IC numbers colored red indicate increased apoptosis in comparison to in *GMR>Cindr^{RNAi}* retinas. Those colored green indicate less apoptosis.
2. Two sample T-tests compared IC number in experimental and *GMR>Cindr^{RNAi}* retinas: all showed a significant change in IC number.

Table 3
Quantification of IC number in retinas at 40 h APF when JNK signaling was compromised (N=75).[a]

GENOTYPE	IC number per data point	
	Mean	SD
GMR > lacZ	**12.30**	0.58
GMR > msn$^{RNAi\text{-}JF03219}$	**12.11**	0.64
GMR > slpr^{KD}	**12.21**	0.49
GMR > hep$^{RNAi\text{-}GL00089}$	**12.34**	1.01
GMR > bsk$^{RNAi\text{-}GL00431}$	**12.51**	0.79
GMR > bsk$^{RNAi\text{-}JF01275}$	**12.30**	0.78
GMR > bsk^{DN}	**12.13**	0.74
GMR > puc	**12.00**	0.37
GMR > jun$^{RNAi\text{-}JF01184}$	**12.15**	0.59

[a] The mean IC numbers of all genotypes listed did not differ significantly from that of control *GMR > lacZ* retinas.

activity detected across entire retinas; see Methods) revealed that the amount and severity of apoptosis was qualitatively equivalent at 18 and 21 h APF in *GMR > lacZ* retina, declined at 24 h APF, and then increased modestly in intensity at 27 h APF (Fig. 2A and B, Fig. S3A, Fig. S4A, Fig. S5A).

Reducing *cindr* resulted in fewer cells populating retinas even at 18 h APF (Fig. 3A and B), but apoptosis and cell proliferation were unchanged in third larval instar eye discs expressing *cindr^{RNAi}* (Fig. S6), suggesting that apoptosis begins prematurely in *GMR > cindr^{RNAi}* pupae. We began our analyses of cell death at 18 h APF, however, as dissecting pupae without damaging the retina prior to this age is technically very difficult, and because the major morphogenetic events that pattern the retina begin from around this age. At 18 h APF, the severity of apoptosis (indicated by Dcp-1 activity) was not markedly changed by *cindr^{RNAi}* expression (Fig. 2A). However, by 21 h APF many *GMR > cindr^{RNAi}* retinas were marked by severe apoptosis (Fig. 2A, Fig. S4). Death subsided modestly at 24 h APF and then increased again at 27 h APF (Fig. 2A and E, Fig. S5D, Fig. 3). Few cells were removed after 30 h APF. Hence the pattern of cell death in *GMR > cindr^{RNAi}* retinas mimicked that of *GMR > lacZ* retinas but with two important differences. First, cell death began early. Second, a larger number of cells were pruned per data point from 18 to 21 h APF (1.80 cells when *cindr* was reduced as opposed to 0.97 in control *lacZ*-expressing retinas, Table 1). Hence we conclude that Cindr is especially important to protect cells from death during this early developmental period. Interestingly, reducing Cindr did not modify the deceleration of apoptosis that began from ~30 h APF, suggesting that a 'breaking mechanism' that halts cell death is independent of Cindr.

Ectopic *bsk* expression also reduced the number of cells populating retinas at 18 h APF (Fig. 3) but only modestly increased apoptosis observed at 18, 21, 24 and 27 h APF (Fig. 2A and C, Fig. S3B, Fig. S4B and Fig. S5B). However, after 27 h APF, cell death reduced and the number of ICs populating the lattice at 40 h APF was normal (Table 1, Fig. 3, Fig. 4B). These data indicate that the 'breaking mechanism' limits loss of ICs after 30 h APF overcomes even ectopic *bsk*.

In contrast, ectopic expression of *bsk* in *cindr^{RNAi}*-expressing retinas markedly enhanced apoptosis to reduce the number of cells in retinas (Fig. 2A and F, Fig. S3E, Fig. S4E and Fig. S5E). Further, cell death was reduced in *bsk$^{1/+}$, cindr^{RNAi}* retina (Fig. 2A and G, Fig. S3F, Fig. S4F and Fig. S5F), although the number of cells within these retinas was also reduced at 18 h APF (Fig. 3; again cell death was unperturbed in the larval eye, Fig. S6). Indeed the mean number of cells lost, per data point, was reduced to 0.72 cell from 18 and 21 h APF, and to 1.43 cells from 21 to 24 h APF in *bsk$^{1/+}$, cindr^{RNAi}* retina, in comparison to 1.80 and 1.58 cells in *cindr^{RNAi}* retina during these same time intervals (Table 1). Taken together, these data support the hypothesis that Cindr protects ICs from JNK-mediated apoptosis.

3.4. Modifying JNK activity changes the final number of ICs in GMR > cindr^{RNAi} retinas

To confirm that JNK signaling activity mediates death of ICs when *cindr^{RNAi}* transgenes are expressed, we extended our analyses to include additional *bsk* alleles and alleles of additional components of the JNK pathway. This time we restricted our analyses to examining only the number of ICs within retinas at 40 h APF (Fig. 4, Fig. S8, Table 2). As before, ectopic *bsk* in *GMR > cindr^{RNAi}* retinas severely reduced the number of ICs (Fig. 4C and D), whilst mutations in the kinases *msn*, *slpr*, *hep*, and *bsk,* as well as the transcription factors *jun* and/or *fos* increased the number of ICs in *GMR > cindr^{RNAi}* retinas (Fig. 4E to P, Table 2). Partial suppression of the *cindr^{RNAi}*-induced cell death indicates that Cindr interacts with additional molecular mechanisms that are independent of JNK signaling to protect ICs from apoptosis.

3.5. At least some JNK activity is required during apoptosis of ICs

Surprisingly, mutations in *slpr* and *bsk* increased the number of ICs in *GMR > cindr^{RNAi}* to above the usual wild type number of 12. These observations led us to question whether JNK activity made at least a minor contribution to normal IC apoptosis – this activity might have been compromised in *slpr* and *bsk* heterozygotes. Indeed, although the number of cells removed from *bsk$^{1/+}$* retinas between 18 and 40 h APF (an average loss of 7.18 cells per data point) was similar to the number of cells removed in control *GMR > lacZ* retinas (7.36 cells per data point, Table 1), the severity of Dcp-1 activity revealed a modest delay in significant pruning of ICs (Fig. 2A). Reducing expression or function of the JNK kinases or Jun or Fos during pupal development lead to occasional extra ICs at 40 h APF (Fig. S9), although the average number of ICs observed across entire retinas was not significantly modified (Table 3). We conclude that at least some JNK activity is required for the normal progression of apoptosis in the eye field and that some JNK activity escapes repression to enhance efficient removal of ICs, although JNK is not a prominent driver of IC death. Our experimental approach, however, has not addressed whether other apoptosis-inducing mechanisms function redundantly with JNK to ensure efficient removal of ICs.

3.6. JNK activity contributes to IC intercalation

In addition to reducing the number of ICs within the lattice, reducing expression of *cindr* introduced defects in the arrangement and shape of ICs (Fig. 1D, Fig. 4C). 1° cells and bristle groups were also frequently improperly positioned. These defects distorted the hexagonal lattice and can be quantified as an ommatidial mis-patterning score (OMS) (Table 4) (Johnson and Cagan, 2009). Mutations in JNK pathway components modified the frequency of these patterning defects (Fig. 4E to M, Table 4). Patterning was modestly improved by mutations in *hep*, *jun* and *fos* but mutations in *msn*, *slpr* and *bsk*, which increased the number of ICs to above 12, increased *cindr^{RNAi}*-induced patterning errors. Many ICs failed to adopt the correct positions and shapes: this was especially evident in genotypes characterized by additional cells.

To assess which cell behaviors were modified by interactions between *cindr* and JNK, we examined retinas at 24 h APF expressing *cindr^{RNAi}* in the setting of reduced or compromised *bsk* expression (Fig. 5). In control *GMR > lacZ* retinas, most 1° cells were of comparative size and scalloped in shape, and the ICs had intercalated and arranged into single file between ommatidia by 24 h APF (Fig. 5A). These characteristics were not modified when *bsk* was over-expressed (Fig. 5B) nor in *bsk* heterozygotes (Fig. 5C). In *GMR > cindr^{RNAi}* retinas, 1°s were variable in size and shape, scalloping often less pronounced and some 1° pairs failed to 'seal' properly around the four cone cells (Fig. 5D). In addition, ECad was not distributed about the

Table 4
Quantification of patterning errors (OMS) in retinas at 40 h APF (N=75).

GENOTYPE [1.]	OMS [2.] Mean	SD	p-value [3.]
GMR>lacZ	**0.5**	0.7	n/a
GMR>cindr^{RNAi}	**5.6**	1.9	0.0798
GMR>cindr^{RNAi}, msn$^{102/+}$	**6.2**	2.3	
GMR>cindr^{RNAi}	**5.4**	2.0	0.0212
GMR>cindr^{RNAi}, slpr$^{BS06/+}$	**6.3**	2.6	
GMR>cindr^{RNAi}	**5.8**	2.0	0.0006 *
GMR>cindr^{RNAi}, hep$^{r75/+}$	**4.3**	2.0	
GMR>cindr^{RNAi}	**5.8**	1.9	0.0006 *
GMR>cindr^{RNAi}, bsk$^{1/+}$	**7.7**	2.9	
GMR>cindr^{RNAi}	**5.4**	2.5	2.8 x 10^{-7} *
GMR>cindr^{RNAi}, bsk$^{2/+}$	**8.8**	3.4	
GMR>cindr^{RNAi}	**5.7**	1.9	0.0137
GMR>cindr^{RNAi}, jun$^{76-19/+}$	**3.9**	1.9	
GMR>cindr^{RNAi}	**5.7**	2.1	0.7591
GMR>cindr^{RNAi}, jun$^{A109/+}$	**5.6**	2.4	
GMR>cindr^{RNAi}	**6.1**	1.3	0.0074 *
GMR>cindr^{RNAi}, fos$^{1/+}$	**5.4**	2.0	
GMR>cindr^{RNAi}	**6.0**	1.6	0.3879
GMR>cindr^{RNAi}, fos$^{2/+}$	**6.2**	2.2	
GMR>cindr^{RNAi}	**5.4**	2.0	0.0062 *
GMR>cindr^{RNAi}, jun$^{76-19/+}$, fos$^{1/+}$	**4.8**	2.1	

1. Retinas heterozygous for each of the JNK loci patterned correctly, with only occasional patterning errors that did not differ from those in control *GMR>lacZ* tissue. These data are not shown.
2. The Ommatidial Mispatterning Score (OMS) is the mean number of errors observed in each hexagonal field; SD = standard deviation. Values in red denote enhancement of *GMR>Cindr^{RNAi}* patterning errors; values in green denote partial rescue of errors.
3. Two sample T-tests compared total patterning errors in experimental and *GMR>Cindr^{RNAi}* datasets. P-values indicated by an * are statistically significant at the 1% confidence level.

entire periphery of cells in *GMR > cindr^{RNAi}* retinas, indicating defects in the apical adherens junctions that suggest weakened adhesion between cells. ICs were also large and adopted random shapes in comparison to those in control *GMR > lacZ* retinas (Fig. 5D). These defects were not markedly modified when *bsk* levels were modified (Fig. 5E and F). However, reducing *bsk* in *GMR > cindr^{RNAi}* retinas modified the arrangement of ICs, which remained grouped rather than positioned in single file in many places between ommatidia (Fig. 5F). These patterning defects were not resolved by 40 h APF (Fig. 4H and I). ICs are usually repositioned into single file via intercalation, a process that is mediated by actin and junction remodeling and changes in cell shape and which can occur even when too many ICs populate the lattice (Johnson et al., 2011; Larson et al., 2010). Importantly, errors in cell shape and arrangement were observed in retinas with reduced JNK activity, although these patterning defects were not widespread (Fig. S9). Taken together, these data indicate that JNK activity promotes lattice patterning by fine-tuning IC shape and position.

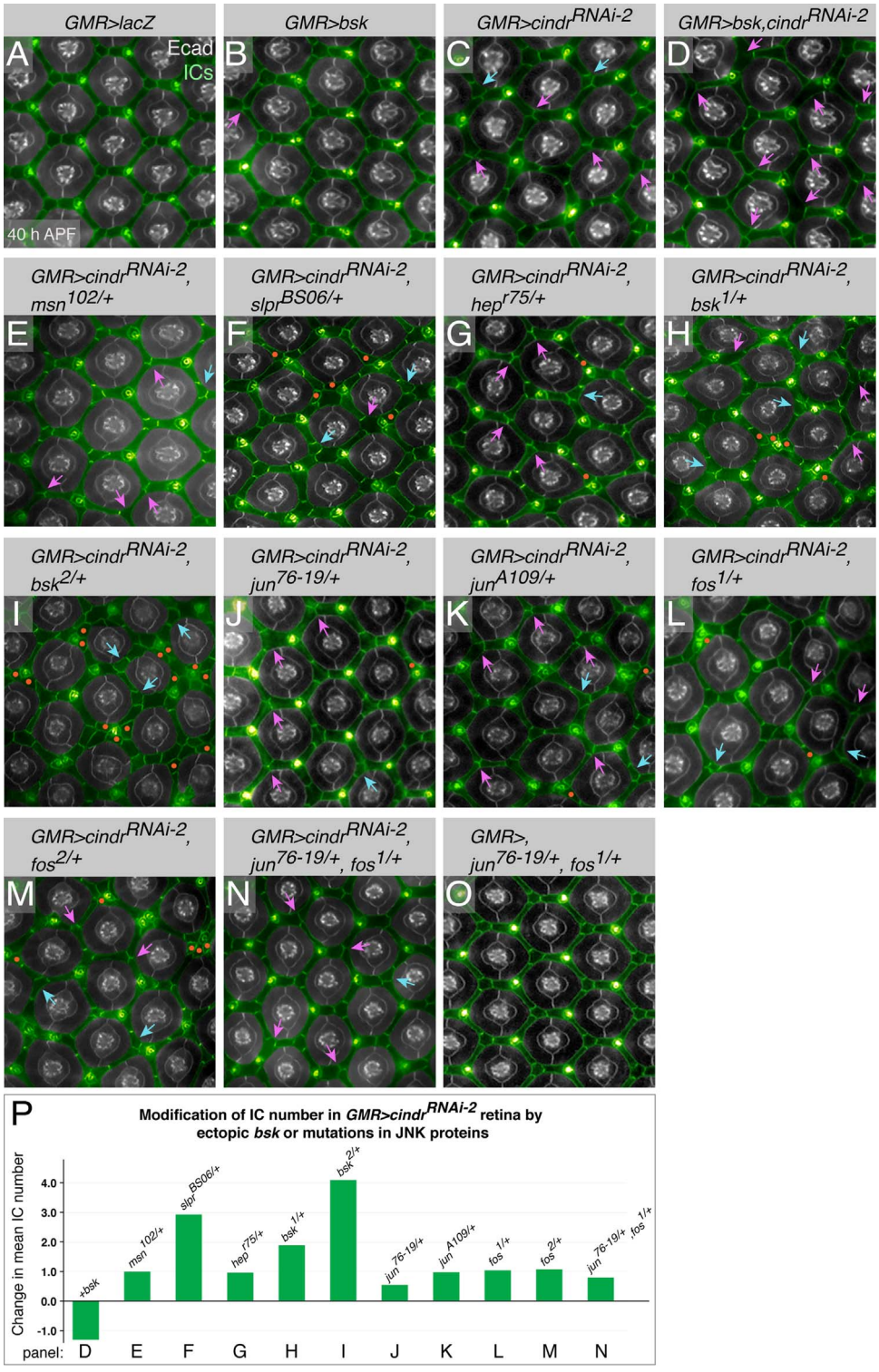

Fig. 4. Components of the JNK signaling pathway modify *GMR > cindr^{RNAi2}* mis-patterning and loss of cells. (A) Small region of a control eye expressing *LacZ*. (B) Over-expression of *bsk* introduced few patterning errors into retinas. The position of a missing 3° is indicated with a pink arrow. (C) *cindr^{RNAi-2}* introduced patterning errors into the IC lattice and led to missing ICs (pink arrows) and incorrectly positioned or shaped 3°s (blue arrows). Only select errors are annotated in this and subsequent panels. Errors in bristle placement and 3° cell arrangement are also present but not annotated. Orange dots indicate examples of ICs that failed to be pruned by apoptosis. Mis-patterning was enhanced by (D) co-expression of *bsk*. Mutations in (E) *msn*, (F) *slpr*, (G) *hep*, (H and I) *bsk*, (J and K) *jun* or (L and M) *fos*, and (N) both *jun* and *fos* modified the patterning errors and the number of ICs in *cindr^{RNAi-2}* retinas. Retinas heterozygous for (O) the *GMR-Gal4* driver and *jun* and *fos* or any of the other JNK signaling loci (not shown) were correctly patterned with the correct number of ICs. (P) Plot of the change in mean IC number in retinas of genotypes corresponding to panels D to N, relative to the mean number of ICs in *GMR > cindr^{RNAi-2}* eyes. All genotypes were dissected at 40 h APF. ICs have been pseudo-colored green. All image panels are presented in Fig. S8 without annotations.

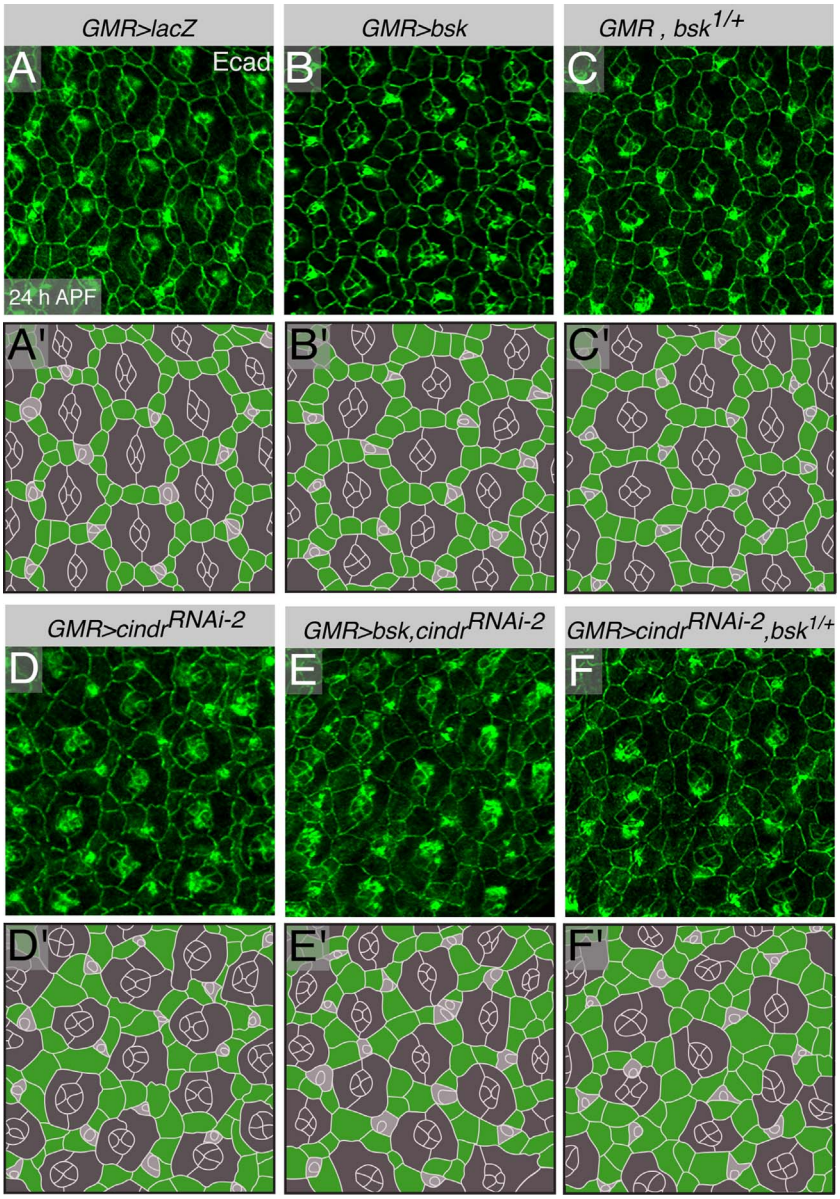

Fig. 5. Eye mis-patterning when *cindr* and *bsk* are modified is evident in young pupal retinas. (A) Control *GMR > lacZ* retina at 24 h APF. The honey-comb lattice that is already evident is largely unmodified by (B) ectopic *bsk* or in (C) retinas heterozygous for *bsk*. (D) The lattice is severely disrupted by $cindr^{RNAi\text{-}2}$ expression. ICs are large and irregularly shaped. Modification of lattice mis-patterning is not yet evident in (E) retinas co-expressing *bsk* with $cindr^{RNAi}$. (F) In *bsk* heterozygotes with $cindr^{RNAi}$ expression, many ICs fail to resolve into single file but remain grouped. All genotypes were dissected at 24 h APF. ECadherin is shown in green. Tracings of each image are presented in panels A' to F', with ICs in green, cone and 1° cells in dark grey and bristle groups in light grey.

3.7. How does Cindr inhibit JNK signaling?

We have previously co-immunoprecipitated Cindr and Bsk from *Drosophila* embryos (Yasin et al., 2016), suggesting that these form a complex *in vivo*. Hence we hypothesized that Cindr could recruit ubiquitin-conjugating enzymes to direct Bsk degradation or recruit a phosphatase to trigger Bsk inactivation.

To test these hypotheses, we over-expressed Cindr in the embryo using *daughterless-GAL4* or in the larval wing with *c765-GAL4*. Despite an eight-fold increase in Cindr in the wing (mean=7.95 fold increase, SD=2.13) and 13-fold increase in the embryo (mean=12.79 fold increase, SD=4.84), Bsk decreased by an average of only 7% in embryo and 12% in wing lysates (Fig. 6A to D). Phosphorylated Bsk similarly decreased by only 8% in wing discs (Fig. 6C to D). In addition, RNAi transgenes that reduced the availability of Cindr by up to 61% (SD=13%) did not significantly modify the amount of Bsk in embryos (Fig. 6A and B). Reducing *cindr* through the entire wing disc led to widespread cell death, precluding further analysis of this tissue. Given these modest changes in Bsk concentration and phosphorylation, it is unlikely that Cindr limits JNK signaling by regulating the amount or phosphorylation state of Bsk.

4. Conclusions

Our genetic data indicate that the conserved adaptor protein Cindr antagonizes JNK signaling in the pupal eye. This interaction is crucial to protect the interommatidial cell lattice from rampant apoptosis during development. Hence Cindr contributes to the mechanism that ensures an appropriate number of cells populate the honeycomb lattice to correctly pattern the eye field.

Our experimental strategies also uncovered a minor role for JNK in fine-tuning the shapes and positions of ICs. That JNK contributes to IC shape is consistent with JNK's well-characterized role in regulating cell shape in other developmental contexts. For example, during dorsal

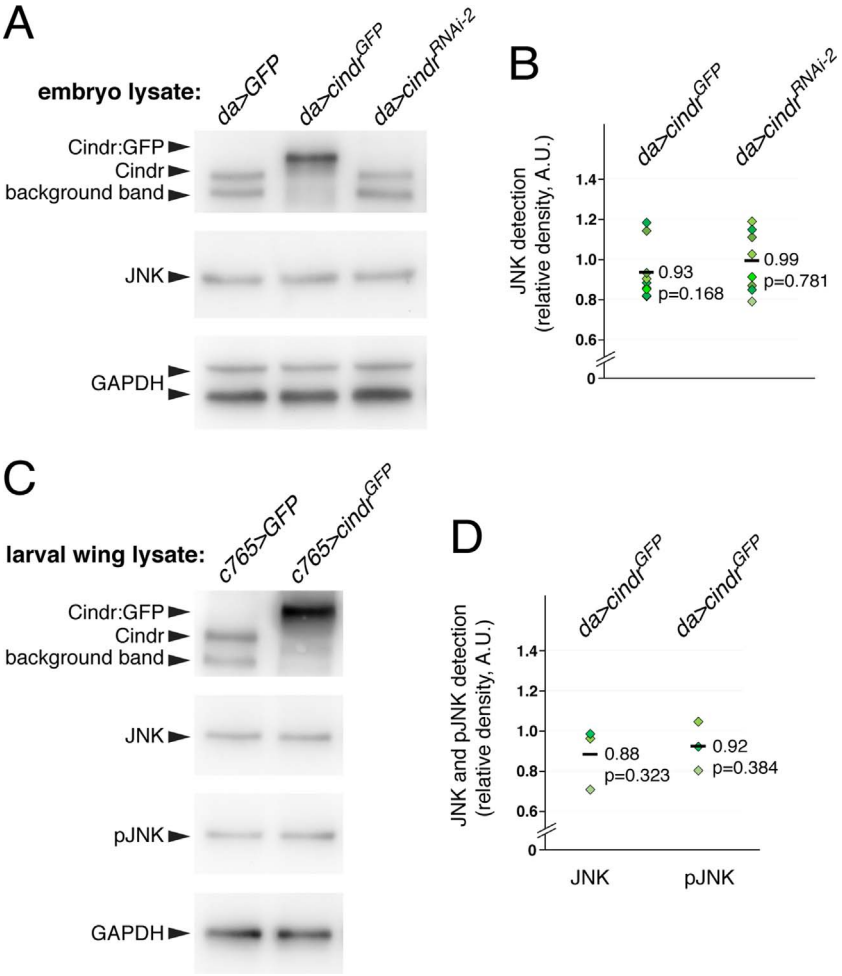

Fig. 6. Cindr neither regulates concentrations of Bsk nor its phosphorylation. (A) Representative Western Blot detecting Cindr (top panel), JNK (middle panel) and GAPDH (bottom panel, loading control) in lysate gathered from embryos expressing ectopic *GFP*, *cindr* or *cindr*^{RNAi}. One-fifth of the amount of *da > cindr* lysate was loaded for the blot to be probed with anti-Cindr: endogenous Cindr was therefore not detected in this lane. (B) Plot of the amount of JNK (diamonds) within each experimental lysate, relative to the amount of JNK in control *da > GFP* lysate, measured via densitrometry analyses of Western Blots of each lysate sample. The mean amount of JNK is indicated (horizontal bars) together with students *t*-test p values. (C) Representative Western Blot detecting Cindr (top panel), JNK (2nd panel), activated pJNK (3rd panel) and GAPDH (bottom panel) in lysate of larval wings expressing ectopic *GFP* or *cindr*. As before, one-fifth of the amount of *c765 > cindr* lysate was loaded for the gels/blots probed with anti-Cindr. (D) Plot of JNK and pJNK detected in *c765 > cindr* wings, relative to the amount of these proteins in *c765 > GFP* wings. Analyses of three independent wing samples are shown, together with the mean amount of JNK or pJNK (horizontal bars). The antibody to GAPDH recognized two species in embryo lysates and one in larval wing samples.

closure in the *Drosophila* embryo, JNK activity in the single row of lateral leading edge cells causes cells to elongate, contributing to the stretching of the lateral epithelial sheets to cover the amnioserosa and seal the embryo (Rios-Barrera and Riesgo-Escovar, 2013; Stronach, 2005). JNK similarly drives cell elongation during closure of the Drosophila thorax. In addition, genetic manipulations that activate JNK can profoundly alter the shapes of epithelial cells: for example, activating JNK in the peripodial membrane causes these hexagonal cells to elongate (Tripura et al., 2011). Additional experiments are required to determine whether JNK activity similarly contributes to shaping the epithelial cells of the developing fly pupal eye. In particular, live-imaging studies will be needed to ascertain whether JNK contributes to cell elongations that drive the intercalation of interommatidial cells from multiple to single rows (Hellerman et al., 2015). On the other hand, JNK activity has also been implicated in regulating adhesive junctions (Llense and Martin-Blanco, 2008; Wang et al., 2010) and it is possible that JNK activity reinforces adhesion during or after IC intercalation. A similar role has been ascribed to JNK during mammalian gut elongation (Dush and Nascone-Yoder, 2013).

The mechanism by which Cindr antagonizes JNK signaling remains to be resolved. Cindr and Bsk interact *in vivo* (these co-immunoprecipitate from *Drosophila* embryos) and interactions between Cindr and Bsk have been detected in two yeast 2-hybrid screens (Giot et al., 2003; Stanyon et al., 2004; Yasin et al., 2016). These data imply that Cindr complexes with Bsk in epithelia. Because Cindr lacks enzymatic activity, we hypothesized that appropriate enzymes are recruited to Cindr-Bsk complexes to regulate the Bsk kinase. However, our biochemical analyses do not support a model in which Cindr promotes JNK degradation via recruitment of the ubiquitin ligase machinery. Similarly, it is unlikely that Cindr promotes JNK inactivity via recruitment of a phosphatase. Instead, we propose that Cindr may modulate activity of the JNK pathway by sequestering Bsk away from its effector targets including the AP-1 transcription factors. Alternatively, Cindr may simply out-compete the AP-1 proteins in their quest to bind activated Bsk.

Cindr is richly expressed in *Drosophila* tissues and we therefore suggest that Cindr provides a general and effective mechanism to limit JNK signaling that might otherwise severely modify tissue morphology and function. Indeed, in our genetic analyses, ectopic expression of *bsk* was insufficient to induce JNK activity unless expression of *cindr* was reduced. Since we have observed similar control of JNK by Cindr in the developing wing epithelium (Yasin et al., 2016), we hypothesize that Cindr is a general regulator of JNK activity. How then do the JNK kinases overcome Cindr's repression in order to trigger signaling in the

different developmental contexts that require JNK? In the *Drosophila* pupal retina, it is possible that the TNF receptor ligand *eiger* is spatially and temporally expressed and triggers high levels of JNK activity that momentarily overcomes Cindr repression. Alternatively, Cindr is modified, displaced or sequestered, releasing JNK from its inhibitory grip.

Besides antagonizing JNK to promote IC survival, Cindr fulfills other important roles in tissues, including regulation of the cytoskeleton, junctions, vesicular trafficking and cytokinesis (Eikenes et al., 2013; Haglund et al., 2010; Johnson et al., 2012, 2011, 2008; Quinones et al., 2010). Indeed, Cindr contains a variety of interaction motifs to facilitate protein interactions but few of these interactions have been well-characterized. In this manuscript we describe that reducing expression of the Cindr isoforms containing the N-terminal SH3 domains impaired the survival of retinal ICs (although as discussed, additional patterning defects, independent of IC number, were also evident). Our data implies that Bsk is amongst the proteins that dock with these Cindr isoforms to influence cell death/survival decisions. However, our data also implies that other signals, independent of JNK, also interact to modify the survival or death of retinal cells.

The vertebrate ortholog of Cindr, CD2AP, is also important for cell survival, but this has been ascribed to PI3-K/Akt signaling and TGF-β activity (Asanuma et al., 2007; Huber et al., 2003; Schiffer et al., 2004) Whether Cindr regulates the orthologous signals in the *Drosophila* pupal eye remains to be investigated. Similarly, whether CD2AP also limits JNK signaling in vertebrate cells requires investigation. Additionally, variants of *CD2AP* have been associated with susceptibility to Alzheimer disease (Chouraki and Seshadri, 2014; Karch and Goate, 2015). Experimental data indicates that CD2AP protects neurons from Tau-mediated toxicity (Shulman et al., 2013, 2014). Whether this is because CD2AP protects neurons from JNK-mediated apoptosis deserves testing.

Acknowledgements

We thank colleagues and the Bloomington *Drosophila* Stock Center (NIH P40OD018537) for many fly strains used in this study. This work was supported by laboratory start-up funds and project grants awarded by Wesleyan University and by R15GM114729 awarded by the NIGMS.

Appendix A. Supporting information

Supplementary data associated with this article can be found in the online version at doi:10.1016/j.ydbio.2017.11.002.

References

Asanuma, K., Campbell, K.N., Kim, K., Faul, C., Mundel, P., 2007. Nuclear relocation of the nephrin and CD2AP-binding protein dendrin promotes apoptosis of podocytes. Proc. Natl. Acad. Sci. USA 104, 10134–10139.
Baker, N.E., Yu, S.Y., 2001. The EGF receptor defines domains of cell cycle progression and survival to regulate cell number in the developing Drosophila eye. Cell 104, 699–708.
Bergmann, A., Agapite, J., McCall, K., Steller, H., 1998. The Drosophila gene hid is a direct molecular target of Ras-dependent survival signaling. Cell 95, 331–341.
Bergmann, A., Tugentman, M., Shilo, B.Z., Steller, H., 2002. Regulation of cell number by MAPK-dependent control of apoptosis: a mechanism for trophic survival signaling. Dev. Cell 2, 159–170.
Betz, A., Ryoo, H.D., Steller, H., Darnell, J.E., Jr., 2008. STAT92E is a positive regulator of Drosophila inhibitor of apoptosis 1 (DIAP/1) and protects against radiation-induced apoptosis. Proc. Natl. Acad. Sci. USA 105, 13805–13810.
Bogler, O., Furnari, F.B., Kindler-Roehrborn, A., Sykes, V.W., Yung, R., Huang, H.J., Cavenee, W.K., 2000. SETA: a novel SH3 domain-containing adapter molecule associated with malignancy in astrocytes. Neuro-Oncol. 2, 6–15.
Brodsky, M.H., Nordstrom, W., Tsang, G., Kwan, E., Rubin, G.M., Abrams, J.M., 2000. Drosophila p53 binds a damage response element at the reaper locus. Cell 101, 103–113.
Cagan, R., 1993. Cell fate specification in the developing Drosophila retina. Dev. Suppl., 19–28.
Cagan, R.L., Ready, D.F., 1989a. The emergence of order in the Drosophila pupal retina. Dev. Biol. 136, 346–362.
Cagan, R.L., Ready, D.F., 1989b. Notch is required for successive cell decisions in the developing Drosophila retina. Genes Dev. 3, 1099–1112.
Cha, G.H., Cho, K.S., Lee, J.H., Kim, M., Kim, E., Park, J., Lee, S.B., Chung, J., 2003. Discrete functions of TRAF1 and TRAF2 in Drosophila melanogaster mediated by c-Jun N-terminal kinase and NF-kappaB-dependent signaling pathways. Mol. Cell Biol. 23, 7982–7991.
Chen, P., Nordstrom, W., Gish, B., Abrams, J.M., 1996. grim, a novel cell death gene in Drosophila. Genes Dev. 10, 1773–1782.
Chen, P., Rodriguez, A., Erskine, R., Thach, T., Abrams, J.M., 1998. Dredd, a novel effector of the apoptosis activators reaper, grim, and hid in Drosophila. Dev. Biol. 201, 202–216.
Chen, W., White, M.A., Cobb, M.H., 2002. Stimulus-specific requirements for MAP3 kinases in activating the JNK pathway. J. Biol. Chem. 277, 49105–49110.
Chouraki, V., Seshadri, S., 2014. Genetics of Alzheimer's disease. Adv. Genet. 87, 245–294.
Cordero, J., Jassim, O., Bao, S., Cagan, R., 2004. A role for wingless in an early pupal cell death event that contributes to patterning the Drosophila eye. Mech. Dev. 121, 1523–1530.
Craige, S.M., Reif, M.M., Kant, S., 2016. Mixed - Lineage Protein kinases (MLKs) in inflammation, metabolism, and other disease states. Biochim. Biophys. Acta 1862, 1581–1586.
Dorstyn, L., Colussi, P.A., Quinn, L.M., Richardson, H., Kumar, S., 1999. DRONC, an ecdysone-inducible Drosophila caspase. Proc. Natl. Acad. Sci. USA 96, 4307–4312.
Dush, M.K., Nascone-Yoder, N.M., 2013. Jun N-terminal kinase maintains tissue integrity during cell rearrangement in the gut. Development 140, 1457–1466.
Dustin, M.L., Olszowy, M.W., Holdorf, A.D., Li, J., Bromley, S., Desai, N., Widder, P., Rosenberger, F., van der Merwe, P.A., Allen, P.M., Shaw, A.S., 1998. A novel adaptor protein orchestrates receptor patterning and cytoskeletal polarity in T-cell contacts. Cell 94, 667–677.
Eikenes, A.H., Brech, A., Stenmark, H., Haglund, K., 2013. Spatiotemporal control of Cindr at ring canals during incomplete cytokinesis in the Drosophila male germline. Dev. Biol. 377, 9–20.
Faul, C., Asanuma, K., Yanagida-Asanuma, E., Kim, K., Mundel, P., 2007. Actin up: regulation of podocyte structure and function by components of the actin cytoskeleton. Trends Cell Biol. 17, 428–437.
Fraser, A.G., Evan, G.I., 1997. Identification of a Drosophila melanogaster ICE/CED-3-related protease, drICE. EMBO J. 16, 2805–2813.
Fraser, A.G., McCarthy, N.J., Evan, G.I., 1997. drICE is an essential caspase required for apoptotic activity in Drosophila cells. EMBO J. 16, 6192–6199.
Fuchs, Y., Steller, H., 2011. Programmed cell death in animal development and disease. Cell 147, 742–758.
Fuchs, Y., Steller, H., 2015. Live to die another way: modes of programmed cell death and the signals emanating from dying cells. Nat. Rev. Mol. Cell Biol. 16, 329–344.
Giot, L., Bader, J.S., Brouwer, C., Chaudhuri, A., Kuang, B., Li, Y., Hao, Y.L., Ooi, C.E., Godwin, B., Vitols, E., Vijayadamodar, G., Pochart, P., Machineni, H., Welsh, M., Kong, Y., Zerhusen, B., Malcolm, R., Varrone, Z., Collis, A., Minto, M., Burgess, S., McDaniel, L., Stimpson, E., Spriggs, F., Williams, J., Neurath, K., Ioime, N., Agee, M., Voss, E., Furtak, K., Renzulli, R., Aanensen, N., Carrolla, S., Bickelhaupt, E., Lazovatsky, Y., DaSilva, A., Zhong, J., Stanyon, C.A., Finley, R.L., Jr., White, K.P., Braverman, M., Jarvie, T., Gold, S., Leach, M., Knight, J., Shimkets, R.A., McKenna, M.P., Chant, J., Rothberg, J.M., 2003. A protein interaction map of Drosophila melanogaster. Science 302, 1727–1736.
Glise, B., Bourbon, H., Noselli, S., 1995. hemipterous encodes a novel Drosophila MAP kinase kinase, required for epithelial cell sheet movement. Cell 83, 451–461.
Gout, I., Middleton, G., Adu, J., Ninkina, N.N., Drobot, L.B., Filonenko, V., Matsuka, G., Davies, A.M., Waterfield, M., Buchman, V.L., 2000. Negative regulation of PI 3-kinase by Ruk, a novel adaptor protein. EMBO J. 19, 4015–4025.
Goyal, L., McCall, K., Agapite, J., Hartwieg, E., Steller, H., 2000. Induction of apoptosis by Drosophila reaper, hid and grim through inhibition of IAP function. EMBO J. 19, 589–597.
Grether, M.E., Abrams, J.M., Agapite, J., White, K., Steller, H., 1995. The head involution defective gene of Drosophila melanogaster functions in programmed cell death. Genes Dev. 9, 1694–1708.
Haglund, K., Nezis, I.P., Lemus, D., Grabbe, C., Wesche, J., Liestol, K., Dikic, I., Palmer, R., Stenmark, H., 2010. Cindr interacts with anillin to control cytokinesis in Drosophila melanogaster. Curr. Biol. 20, 944–950.
Hawkins, C.J., Wang, S.L., Hay, B.A., 1999. A cloning method to identify caspases and their regulators in yeast: identification of Drosophila IAP1 as an inhibitor of the Drosophila caspase DCP-1. Proc. Natl. Acad. Sci. USA 96, 2885–2890.
Hay, B.A., Wassarman, D.A., Rubin, G.M., 1995. Drosophila homologs of baculovirus inhibitor of apoptosis proteins function to block cell death. Cell 83, 1253–1262.
Hellerman, M.B., Choe, R.H., Johnson, R.I., 2015. Live-imaging of the Drosophila pupal eye. J. Vis. Exp., 52120.
Hotamisligil, G.S., Davis, R.J., 2016. Cell signaling and stress responses. Cold Spring Harb. Perspect. Biol., 8.
Huang, J., Wu, S., Barrera, J., Matthews, K., Pan, D., 2005. The Hippo signaling pathway coordinately regulates cell proliferation and apoptosis by inactivating Yorkie, the Drosophila Homolog of YAP. Cell 122, 421–434.
Huber, T.B., Hartleben, B., Kim, J., Schmidts, M., Schermer, B., Keil, A., Egger, L., Lecha, R.L., Borner, C., Pavenstadt, H., Shaw, A.S., Walz, G., Benzing, T., 2003. Nephrin and CD2AP associate with phosphoinositide 3-OH kinase and stimulate AKT-dependent signaling. Mol. Cell Biol. 23, 4917–4928.
Inoue, H., Tateno, M., Fujimura-Kamada, K., Takaesu, G., Adachi-Yamada, T., Ninomiya-Tsuji, J., Irie, K., Nishida, Y., Matsumoto, K., 2001. A Drosophila MAPKKK, D-MEKK1, mediates stress responses through activation of p38 MAPK. EMBO J. 20, 5421–5430.

Jiang, C., Lamblin, A.F., Steller, H., Thummel, C.S., 2000. A steroid-triggered transcriptional hierarchy controls salivary gland cell death during Drosophila metamorphosis. Mol. Cell 5, 445–455.
Johnson, R.I., Bao, S., Cagan, R.L., 2012. Interactions between Drosophila IgCAM adhesion receptors and cindr, the Cd2ap/Cin85 ortholog. Dev. Dyn. 241, 1933–1943.
Johnson, R.I., Cagan, R.L., 2009. A quantitative method to analyze Drosophila pupal eye patterning. PLoS One 4, e7008.
Johnson, R.I., Sedgwick, A., D'Souza-Schorey, C., Cagan, R.L., 2011. Role for a Cindr-Arf6 axis in patterning emerging epithelia. Mol. Biol. Cell 22, 4513–4526.
Johnson, R.I., Seppa, M.J., Cagan, R.L., 2008. The Drosophila CD2AP/CIN85 orthologue Cindr regulates junctions and cytoskeleton dynamics during tissue patterning. J. Cell Biol. 180, 1191–1204.
Karch, C.M., Goate, A.M., 2015. Alzheimer's disease risk genes and mechanisms of disease pathogenesis. Biol. Psychiatry 77, 43–51.
Kawachi, H., Miyauchi, N., Suzuki, K., Han, G.D., Orikasa, M., Shimizu, F., 2006. Role of podocyte slit diaphragm as a filtration barrier. Nephrology 11, 274–281.
Kirsch, K.H., Georgescu, M.M., Ishimaru, S., Hanafusa, H., 1999. CMS: an adapter molecule involved in cytoskeletal rearrangements. Proc. Natl. Acad. Sci. USA 96, 6211–6216.
Kowanetz, K., Husnjak, K., Holler, D., Kowanetz, M., Soubeyran, P., Hirsch, D., Schmidt, M.H., Pavelic, K., De Camilli, P., Randazzo, P.A., Dikic, I., 2004. CIN85 associates with multiple effectors controlling intracellular trafficking of epidermal growth factor receptors. Mol. Biol. Cell 15, 3155–3166.
Kurada, P., White, K., 1998. Ras promotes cell survival in Drosophila by downregulating hid expression. Cell 95, 319–329.
Kuranaga, E., Kanuka, H., Igaki, T., Sawamoto, K., Ichijo, H., Okano, H., Miura, M., 2002. Reaper-mediated inhibition of DIAP1-induced DTRAF1 degradation results in activation of JNK in Drosophila. Nat. Cell Biol. 4, 705–710.
Larson, D.E., Johnson, R.I., Swat, M., Cordero, J.B., Glazier, J.A., Cagan, R.L., 2010. Computer simulation of cellular patterning within the Drosophila pupal eye. PLoS Comput. Biol. 6, e1000841.
Lehtonen, S., Ora, A., Olkkonen, V.M., Geng, L., Zerial, M., Somlo, S., Lehtonen, E., 2000. In vivo interaction of the adapter protein CD2-associated protein with the type 2 polycystic kidney disease protein, polycystin-2. J. Biol. Chem. 275, 32888–32893.
Lisi, S., Mazzon, I., White, K., 2000. Diverse domains of thread/DIAP1 are required to inhibit apoptosis induced by reaper and HID in Drosophila. Genetics 154, 669–678.
Liu, H., Su, Y.C., Becker, E., Treisman, J., Skolnik, E.Y., 1999. A Drosophila TNF-receptor-associated factor (TRAF) binds the ste20 kinase Misshapen and activates Jun kinase. Curr. Biol. 9 (101-104).
Llense, F., Martin-Blanco, E., 2008. JNK signaling controls border cell cluster integrity and collective cell migration. Curr. Biol. 18, 538–544.
Luo, X., Puig, O., Hyun, J., Bohmann, D., Jasper, H., 2007. Foxo and Fos regulate the decision between cell death and survival in response to UV irradiation. EMBO J. 26, 380–390.
Martin-Blanco, E., Gampel, A., Ring, J., Virdee, K., Kirov, N., Tolkovsky, A.M., Martinez-Arias, A., 1998. puckered encodes a phosphatase that mediates a feedback loop regulating JNK activity during dorsal closure in Drosophila. Genes Dev. 12, 557–570.
Miller, D.T., Cagan, R.L., 1998. Local induction of patterning and programmed cell death in the developing Drosophila retina. Development 125, 2327–2335.
Monserrate, J.P., Brachmann, C.B., 2007. Identification of the death zone: a spatially restricted region for programmed cell death that sculpts the fly eye. Cell Death Differ. 14, 209–217.
Parks, A.L., Turner, F.R., Muskavitch, M.A., 1995. Relationships between complex Delta expression and the specification of retinal cell fates during Drosophila eye development. Mech. Dev. 50, 201–216.
Quinones, G.A., Jin, J., Oro, A.E., 2010. I-BAR protein antagonism of endocytosis mediates directional sensing during guided cell migration. J. Cell Biol. 189, 353–367.
Riddiford, L.M., 1993. Hormones and Drosophila development. In: Bate, Ma.M.A., A. (Ed.), The Development of Drosophila Melanogaster. Cold Spring Harbor Laboratory Press, Cold Spring Harbor, NY, 899–939.
Riesgo-Escovar, J.R., Jenni, M., Fritz, A., Hafen, E., 1996. The Drosophila Jun-N-terminal kinase is required for cell morphogenesis but not for DJun-dependent cell fate specification in the eye. Genes Dev. 10, 2759–2768.
Ring, J.M., Martinez Arias, A., 1993. puckered, a gene involved in position-specific cell differentiation in the dorsal epidermis of the Drosophila larva. Dev. Suppl., 251–259.
Rios-Barrera, L.D., Riesgo-Escovar, J.R., 2013. Regulating cell morphogenesis: the Drosophila Jun N-terminal kinase pathway. Genesis 51, 147–162.
Robinow, S., Draizen, T.A., Truman, J.W., 1997. Genes that induce apoptosis: transcriptional regulation in identified, doomed neurons of the Drosophila CNS. Dev. Biol. 190, 206–213.
Ryoo, H.D., Bergmann, A., Gonen, H., Ciechanover, A., Steller, H., 2002. Regulation of Drosophila IAP1 degradation and apoptosis by reaper and ubcD1. Nat. Cell Biol. 4, 432–438.
Sathyanarayana, P., Barthwal, M.K., Lane, M.E., Acevedo, S.F., Skoulakis, E.M., Bergmann, A., Rana, A., 2003. Drosophila mixed lineage kinase/slipper, a missing biochemical link in Drosophila JNK signaling. Biochim. Biophys. Acta 1640, 77–84.
Schiffer, M., Mundel, P., Shaw, A.S., Bottinger, E.P., 2004. A novel role for the adaptor molecule CD2-associated protein in transforming growth factor-beta-induced apoptosis. J. Biol. Chem. 279, 37004–37012.
Shlevkov, E., Morata, G., 2012. A dp53/JNK-dependant feedback amplification loop is essential for the apoptotic response to stress in Drosophila. Cell Death Differ. 19, 451–460.
Shulman, J.M., Chen, K., Keenan, B.T., Chibnik, L.B., Fleisher, A., Thiyyagura, P., Roontiva, A., McCabe, C., Patsopoulos, N.A., Corneveaux, J.J., Yu, L., Huentelman, M.J., Evans, D.A., Schneider, J.A., Reiman, E.M., De Jager, P.L., Bennett, D.A., 2013. Genetic susceptibility for Alzheimer disease neuritic plaque pathology. JAMA Neurol. 70, 1150–1157.
Shulman, J.M., Imboywa, S., Giagtzoglou, N., Powers, M.P., Hu, Y., Devenport, D., Chipendo, P., Chibnik, L.B., Diamond, A., Perrimon, N., Brown, N.H., De Jager, P.L., Feany, M.B., 2014. Functional screening in Drosophila identifies Alzheimer's disease susceptibility genes and implicates Tau-mediated mechanisms. Hum. Mol. Genet 23, 870–877.
Silverman, N., Zhou, R., Erlich, R.L., Hunter, M., Bernstein, E., Schneider, D., Maniatis, T., 2003. Immune activation of NF-kappaB and JNK requires Drosophila TAK1. J. Biol. Chem. 278, 48928–48934.
Sluss, H.K., Han, Z., Barrett, T., Goberdhan, D.C., Wilson, C., Davis, R.J., Ip, Y.T., 1996. A JNK signal transduction pathway that mediates morphogenesis and an immune response in Drosophila. Genes Dev. 10, 2745–2758.
Song, Z., McCall, K., Steller, H., 1997. DCP-1, a Drosophila cell death protease essential for development. Science 275, 536–540.
Stanyon, C.A., Liu, G., Mangiola, B.A., Patel, N., Giot, L., Kuang, B., Zhang, H., Zhong, J., Finley, R.L., Jr., 2004. A Drosophila protein-interaction map centered on cell-cycle regulators. Genome Biol. 5, R96.
Stronach, B., 2005. Dissecting JNK signaling, one KKKinase at a time. Dev. Dyn. 232, 575–584.
Stronach, B., Perrimon, N., 2002. Activation of the JNK pathway during dorsal closure in Drosophila requires the mixed lineage kinase, slipper. Genes Dev. 16, 377–387.
Su, Y.C., Treisman, J.E., Skolnik, E.Y., 1998. The Drosophila Ste20-related kinase misshapen is required for embryonic dorsal closure and acts through a JNK MAPK module on an evolutionarily conserved signaling pathway. Genes Dev. 12, 2371–2380.
Szymkiewicz, I., Kowanetz, K., Soubeyran, P., Dinarina, A., Lipkowitz, S., Dikic, I., 2002. CIN85 participates in Cbl-b-mediated down-regulation of receptor tyrosine kinases. J. Biol. Chem. 277, 39666–39672.
Takatsu, Y., Nakamura, M., Stapleton, M., Danos, M.C., Matsumoto, K., O'Connor, M.B., Shibuya, H., Ueno, N., 2000. TAK1 participates in c-Jun N-terminal kinase signaling during Drosophila development. Mol. Cell Biol. 20, 3015–3026.
Take, H., Watanabe, S., Takeda, K., Yu, Z.X., Iwata, N., Kajigaya, S., 2000. Cloning and characterization of a novel adaptor protein, CIN85, that interacts with c-Cbl. Biochem. Biophys. Res. Commun. 268, 321–328.
Teng, X., Toyama, Y., 2011. Apoptotic force: active mechanical function of cell death during morphogenesis. Dev. Growth Differ. 53, 269–276.
Teramoto, H., Coso, O.A., Miyata, H., Igishi, T., Miki, T., Gutkind, J.S., 1996. Signaling from the small GTP-binding proteins Rac1 and Cdc42 to the c-Jun N-terminal kinase/stress-activated protein kinase pathway. A role for mixed lineage kinase 3/protein-tyrosine kinase 1, a novel member of the mixed lineage kinase family. J. Biol. Chem. 271, 27225–27228.
Tossidou, I., Teng, B., Drobot, L., Meyer-Schwesinger, C., Worthmann, K., Haller, H., Schiffer, M., 2010. CIN85/RukL is a novel binding partner of nephrin and podocin and mediates slit diaphragm turnover in podocytes. J. Biol. Chem. 285, 25285–25295.
Tripura, C., Chandrika, N.P., Susmitha, V.N., Noselli, S., Shashidhara, L.S., 2011. Regulation and activity of JNK signaling in the wing disc peripodial membrane during adult morphogenesis in Drosophila. Int. J. Dev. Biol. 55, 583–590.
Vucic, D., Kaiser, W.J., Harvey, A.J., Miller, L.K., 1997. Inhibition of reaper-induced apoptosis by interaction with inhibitor of apoptosis proteins (IAPs). Proc. Natl. Acad. Sci. USA 94, 10183–10188.
Vucic, D., Kaiser, W.J., Miller, L.K., 1998. Inhibitor of apoptosis proteins physically interact with and block apoptosis induced by Drosophila proteins HID and GRIM. Mol. Cell Biol. 18, 3300–3309.
Wang, S.L., Hawkins, C.J., Yoo, S.J., Muller, H.A., Hay, B.A., 1999. The Drosophila caspase inhibitor DIAP1 is essential for cell survival and is negatively regulated by HID. Cell 98, 453–463.
Wang, X., He, L., Wu, Y.I., Hahn, K.M., Montell, D.J., 2010. Light-mediated activation reveals a key role for Rac in collective guidance of cell movement in vivo. Nat. Cell Biol. 12, 591–597.
Warner, S.J., Yashiro, H., Longmore, G.D., 2010. The Cdc42/Par6/aPKC polarity complex regulates apoptosis-induced compensatory proliferation in epithelia. Curr. Biol. 20, 677–686.
White, K., Grether, M.E., Abrams, J.M., Young, L., Farrell, K., Steller, H., 1994. Genetic control of programmed cell death in Drosophila. Science 264, 677–683.
Wilson, R., Goyal, L., Ditzel, M., Zachariou, A., Baker, D.A., Agapite, J., Steller, H., Meier, P., 2002. The DIAP1 RING finger mediates ubiquitination of Dronc and is indispensable for regulating apoptosis. Nat. Cell Biol. 4, 445–450.
Wolff, T., Ready, D.F., 1993. Pattern formation in the Drosophila retina. In: Bate, M., Arias, A.M. (Eds.), The Development of Drosophila Melanogaster. Cold Spring Harbor Laboratory Press, Cold Spring Harbor, 1277–1325.
Yasin, H.W., van Rensburg, S.H., Feiler, C.E., Johnson, R.I., 2016. The adaptor protein Cindr regulates JNK activity to maintain epithelial sheet integrity. Dev. Biol. 410, 135–149.
Yin, V.P., Thummel, C.S., 2005. Mechanisms of steroid-triggered programmed cell death in Drosophila. Semin Cell Dev. Biol. 16, 237–243.
Zeitlinger, J., Kockel, L., Peverali, F.A., Jackson, D.B., Mlodzik, M., Bohmann, D., 1997. Defective dorsal closure and loss of epidermal decapentaplegic expression in Drosophila fos mutants. EMBO J. 16, 7393–7401.